Journal of Petroleum Research and Studies

Open Access
No. 40, September 2023, pp. 126-142

P- ISSN: 2220-5381
E- ISSN: 2710-1096

DOI: http://doi.org/10.52716/jprs.v13i3.709

Mordenite-Type Zeolite from Iraq Sand: Synthesis and Characterization

Abdulla M. Ahmed[1*], Aysar T. Jarullah[1], Hala M. Hussein[2], A. N. Ahmed[1]
[1]Department of Chemical Engineering, College of Engineering, University of Tikrit, Tikrit, Iraq.
[2]Petroleum Research and Development Center, Ministry of Oil, Baghdad, Iraq.
[*]Corresponding Author E-mail: abdullah.m.ahmed43777@st.tu.edu.iq

Received 23/10/2022, Revised 27/11/2022, Accepted 01/12/2022, Published 10/09/2023

Abstract

Mordenite's excellent physical and chemical qualities set it apart from other zeolites with similar applications in industry. Mordenite is frequently produced through hydrothermal processing with TEA+ cations. The best template agent is TEA+ cations, despite the fact that they may lead to a variety of problems, such as the release of toxicity, the high cost of production, the contamination of wastewater, and environmental damage. So, it's important to develop a mordenite synthesis technique that doesn't need an organic template or a cheap template. The mordenite-type zeolites were prepared using sand from the western part of Iraq (Ar-Rutbah). Silica was extracted from Iraqi sand as a silica source and sodium aluminate as a source of alumina Al by using the SOL-GEL method through the hydrothermal technique at temperatures ranging from 23 to 27 °C over a period of 7 days. Analyses such as XRD, BET surface area AFM, FT-IR, and FE-SEM were performed on the sample. The average particle size was 31.9 nm, and the BET surface area was 202.487. XRF detected the ratio of silica to alumina (Si/Al = 4.55), and the exchange of sodium ions for hydrogen ions through ionic exchange is 100%. The micrograph clearly reveals a tiny portion of the crystal band with a flaky habit, while FE-SEM images of synthesized H-MOR show that plates form the majority of the crystals.

Keywords: Zeolite; Nano silica; raw material; mordenite.

1. Introduction:

The treatment of fuels now needs more and more active, selective catalysts in order to enhance its future applications as well as to contribute to reducing environmental influences. Because of the growth of industry and progress in technology, energy and environmental issues have become very important issues in our lives. [1].

Open Access
No. 40, September 2023, pp. 126-142
P- ISSN: 2220-5381
E- ISSN: 2710-1096

Crystalline aluminosilicates have a clearly defined microporous structure. Because of their single-pore topologies, large surface area, excellent acidity, and thermal strength, zeolites are commonly utilized as catalysts in the petroleum and chemical industries.[2, 3]

Mordenite (structural style MOR) is an important zeolite. High-silic, big pore zeolite with a network system collected of traditional 12-member rings 0.65 x 0.7 nm connected by a short side containing 8-member ring pores 0.26 x 0.57 nm parallel to the c-axis and an extra 8-member ring channel 0.34 nm x 0.48 nm equivalent to the b-axis. [4].

Mordenite is a mineral with a crystalline structure and element cell measurements of a =18.121 Å, b = 20.517 Å, and c = 7.544 Å that correspond to the space group. Mordenite is an important industrial zeolite used as a heterogeneous catalyst in a range of chemical reactions, including hydro isomerization, catalytic cracking, dewaxing, dehydration, steam reforming, polymerization, xylene isomerization, and adsorption. [5, 6] Despite the fact that the application of mordenite zeolite is not limited (as noted previously), it is rising annually due to its homogeneous structure, small pore size, flexible framework, large internal surface area, and controlled reactivity. It is also commonly applied in separation and purification processes. [7, 8] Mordenite is a type of high-silica zeolite; its synthesis was originally reported in 1927 by Leonard, and it was confirmed for the first time in 1948 by Barrer.[9]

Mordenite has superior chemical resistance, thermal stability, and the presence of Brønsted and Lewis acid sites, a large pore volume, and a high surface area are noted [10] Mordenite dealumination was typically carried out to raise the Si/Al ratio, so strengthening the acid sites and generating intracrystalline mesopores can be observed . [11, 12]

Usually, a hydrothermal process is used to produce mordenites. The amount of research on the various synthesis components is enormous. Materials such sodium silicate, sodium aluminosilicate, active alumina, silicic acid, shapeless silica, rice shells, sunflower husks, clay, chert rock, sands, and used glasses have all been documented as materials that have been utilized in the manufacturing of mordenites.

Various studies have also been carried out to identify the ideal variables (such as the SiO_2/Al_2O_3 ratio, water content, pH level, and aging period) that have been discovered to possess an important impact on the morphology and crystallization rate of mordenite, wich could improve the energy efficiency.

The mordenite-type zeolites that were produced through a hydrothermal procedure by silica and sodium aluminate as Si and Al resources, respectively. In order to find out what temperature is

Open Access
No. 40, September 2023, pp. 126-142
P- ISSN: 2220-5381
E- ISSN: 2710-1096

necessary to make crystal-like mordenite, a 23 mL Teflon-lined autoclave was heated to several values between 150 and 190 °C. Both silica and sodium aluminate are used as silica and alumina sources in their studies, but in our work, local Iraqi sand is used as a silica source and sodium aluminate is used as an alumina source to generate Mordenite-type zeolite at a temperature of 25±2 °C.

(Klunk et al., 2020)[13] used rice husk ash (RHA) and metakaolin in the absence of an organic template at room temperature through the sol–gel method.

(Li et al., 2018) [14] A millimeter sized sphere-shaped mordenite (MOR) zeolite by good mechanical asset was well prepared through vapor assisted revolution of Na-doped SiO2 spheres. It is shown that the precursor made by vacuum impregnation is necessary for getting a good shape retention.

(Hussain & Mohammed, 2019)[15] Mordenite zeolite was manufactured from prepared nano-silica using a hydrothermal method over three days at 25 °C. SEM presented that the equipped sample crystallized into needle-shaped crystals. The BET surface area and pore size of H-mordenite zeolite were 336.7 m2/g and 2.49 nm, correspondingly. AFM showed that the typical crystal diameter was 111 nm. The Si/Al ratio and ion conversation percentage measured by XRF were 7.544 and 99.62 %, individually.

(Journal and Basic, 2017)[16] Using chert rock as a source of silica, prepare mesoporous mordenite through a hydrothermal method.

(Zhu et al ,2016)[17] Mordenite zeolite was produced by an ultrafast, organic structure-directing agent (OSDA)-free method. According to them, the formation of the mordenite zeolite occurred in 10 minutes, which is much faster than traditional techniques.

(Lankapati et al., 2020) [51] Mordenite zeolite was synthesized from coal fly ash by a seed-assisted synthesis approach and then subjected to hydrothermal, ion exchange, and calcination processes for purification. FZSH was found to have a smaller BET surface area than commercial mordenite (432 m2/g vs. 117 m2/g). Researchers also discovered that the pore volume of FZSH material was smaller than that of commercial mordenite (20 cm3/g), coming in at 0.08 cm3/g. Studies showed that its pore size was much greater than that of commercial mordenite zeolite.

The aim of this study is to prepare nanosilica and mordenite zeolite from cheap local Iraqi materials, which can be used to make catalysts and as an alternative to materials that are made using expensive sources like TEA+ cation.

Open Access
No. 40, September 2023, pp. 126-142
P- ISSN: 2220-5381
E- ISSN: 2710-1096

2. Materials and Methods

2.1 chemical Raw material used

In this work, experiment conducted using the sulfuric acid (H_2SO_4) 98% provided by Sigma Aldrich, sodium hydroxide (NaOH) 99% from Alpha Chemika, sodium aluminate 50–55% from Sigma Aldrich and ammonium chloride 99% from BDH Limited Pool, England are used.

2.2 Iraqi sand

As shown in Table (1) the western part of Iraq (Ar-Rutbah) sand was chosen as a natural source of silica to prepare nano-silica because it is highly silica-content, available in Al-Anbar city, and its selection was dependent on XRF analysis, which was considered to be the best analysis for determining the elements in the material.

Table (1) Analyzing the X-Ray Fluorescence (XRF) of Iraqi Sand

Component	SiO_2	Al_2O_3	CaO	SO_2	MgO	other compounds
Weight %	96.7	1.3	1.18	0.35	0.007	0.463

2.3 Nano silica preparation.

40 grams of local sand were ground in a kitchen grinder and filtered through 45 microns of laboratory mesh to eliminate bigger particles. Sodium hydroxide (NaOH) pellets of about 100 grams are finely ground in a grinder. Local sand and NaOH are mixed and calcined for half an hour at 500 °C to create a sodium silicate sponge. After the silicate has cooled, it is crushed and placed in a conical flask. Using a magnetic stirrer, 500 ml of deionized water is added to silicate at 600 rpm to create a green, homogeneous solution with a pH of 14. The 98% sulfuric acid is added slowly while stirring at 600 rpm until a white gel develops and the pH reaches 2.5. The gel is extracted from the mother solution via filtration using a Buckner funnel and a vacuum pump. After filtration, the product was dried overnight at 110 C in an electrical laboratory drier. The product is then washed with deionized water until its pH reaches 7. By adding a few drops of a 6% $BaCl_2$ solution to 5 ml of liquid filter and observing the precipitation of white $BaSO_4$, you can confirm that SO_4^{-2} is not present and determine whether additional cleaning is required. The solid product is washed and dried at 110 °C overnight, and the end product is nano-silica powder. [18]

Open Access
No. 40, September 2023, pp. 126-142
P- ISSN: 2220-5381
E- ISSN: 2710-1096

The diagram shown in Figure (1) shows the applied procedure for preparing nanosilica.

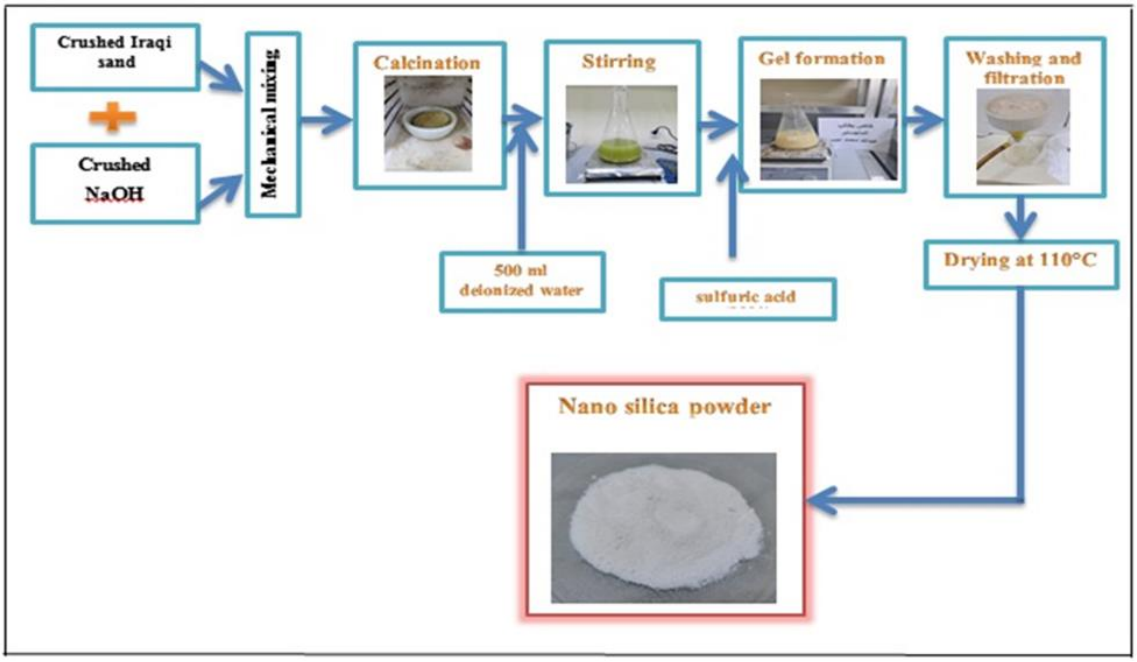

Fig. (1): Flow diagram for Nano silica preparation

2.4 Na-MOR Preparation

dissolved 38.90 grams of NaOH in 249.3 ml of water, then divided into two equal portions. One portion contained 5.56 grams of nano-silica produced from local sand in Iraq. To make a pure aluminate solution, 10.19 g of sodium aluminate $NaAlO_2$ is added to the rest of the solution. At 400 rpm, pouring silicate solution into aluminate solution produced a white, homogenous gel. The gel is stored for seven days at pH 14 in a water bath at (T =25± 2°C) in a sealed laboratory glass bottle with a 200 rpm stirrer. A Buckner funnel and vacuum pump are utilized to filter the solid product The resulting mixture is rinsed with deionized water until the pH value reaches 7. The material was then dried at 110°C for 2 hours before being calcined at 400°C for 2 hours. [14,15]

The following block diagram is shown in Figure (2). It explains the stages for the preparation of Na-MOR.

Open Access
No. 40, September 2023, pp. 126-142
P- ISSN: 2220-5381
E- ISSN: 2710-1096

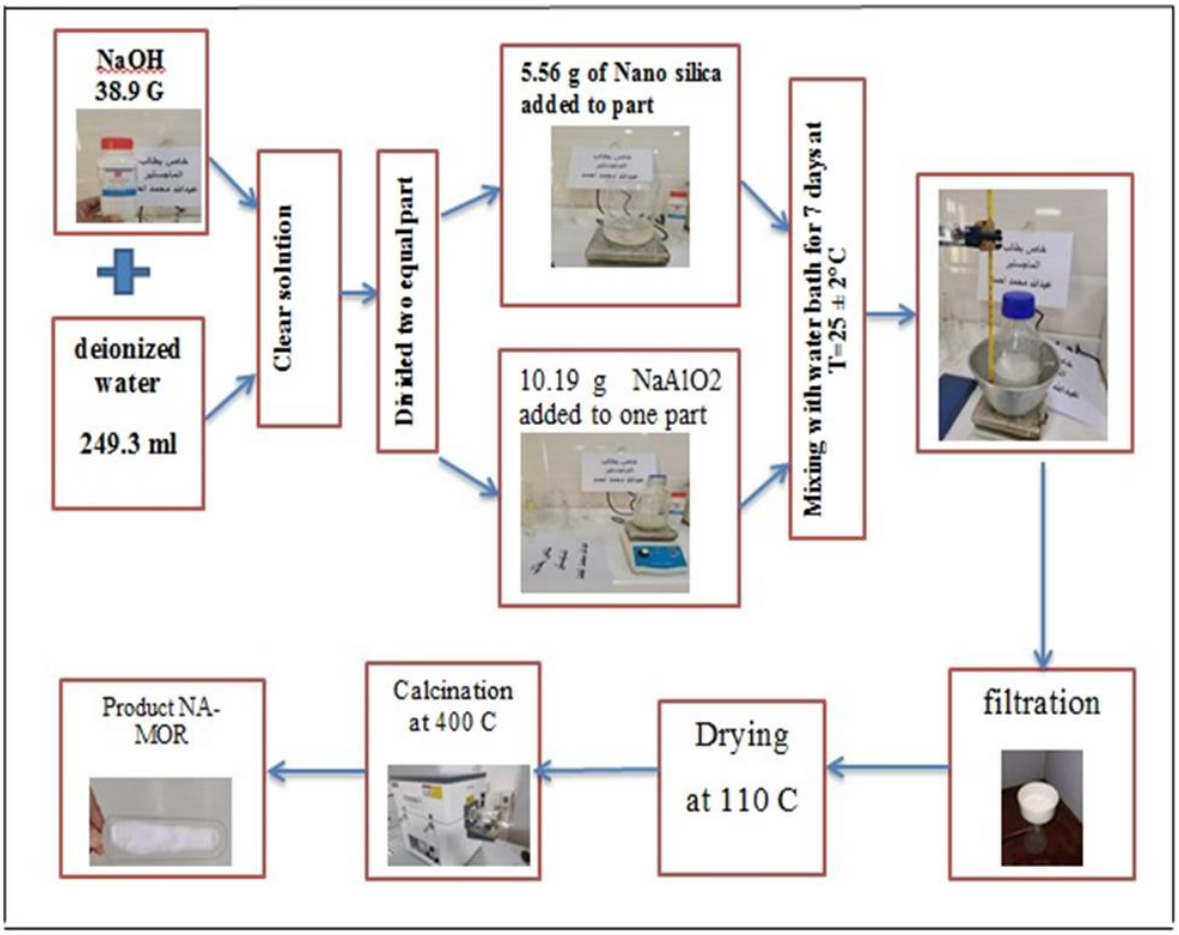

Fig. (2): Schematic flow diagram for synthesizing Na-MOR

2.5 Preparation of (H-MOR)

Zeolite H-MOR was synthesized by exchanging Na-MOR with a 4 N NH_4Cl solution. To complete the ion exchange, Na-MOR zeolite was slurred in an ammonium chloride solution, mixed at 50 °C for 2 hours, and then allowed to rest at room temperature for an additional night. After being stored at room temperature overnight, the product was dried at 110 °C for 2 hours and calcined at 400 °C for another 2 hours.

2.6 characterization

Several methods were used to characterize the samples produced. Scanning electron microscopy (SEM), atomic force microscopy (AFM), X-ray diffraction (XRD), Fourier transform infrared spectroscopy (FTIR), and X-ray fluorescence (XRF) are all examples of such methods. A Philips diffractometer set to a 2 theta value of 5 to 600 was used to measure the XRD of the powdered

Open Access
No. 40, September 2023, pp. 126-142
P- ISSN: 2220-5381
E- ISSN: 2710-1096

product. Estimates of surface area was calculated using the BET (ASAP 2020) model. For this experiment, we used a Perkin-Elmer FTIR (Model 8400S) to scan the IR spectra from 400 to 4000 cm^{-1} using the KBr pellet technique. Quantifying the elements found in the zeolites was accomplished with the use of XRF (Phillips PW 1480 Spectrometer) analysis. Microcrystalline and nanocrystalline zeolite were examined by scanning electron microscopy and atomic force microscopy to determine their particle size and shape. The scanning electron microscope (SEM; VEGA3 LM/SEM) may produce pictures of a sample by scanning it with a focused beam of electrons. Electrons interact with sample electrons to generate detectable signals that provide details about the surface structure and composition of the sample. Information perpendicular and parallel to the surface, down to the nm range, is provided by AFM (SPM-AT 3000).

3. Results and Discussion

3.1 Analyzing of Nano-Silica

3.1.1 BET surface area analysis

The nano-silica that was made from Iraqi sand based on the sol gel process had a surface area of $627 m^2/g$. compared with that by Kadhim et al.[13] with a surface area about $438.215 m^2/g$. This result indicated that the surface area of prepared nano silica is higher than that obtained by previous studies.

3.1.2 XRD Analysis

The nanosilica synthesized from Iraqi sand has an XRD pattern diffractogram shown in Figure (3). The absence of sharp peaks and strong board peaks at 2θ =21.275, which is characteristic of amorphous silica, indicated that the produced nano-silica was totally amorphous. Okoronkwo et al. (2016) [20] create a nano-silica amorphous material from corn cob ash with a 2θ =23 peak, which is close to the result we obtained.

Open Access
No. 40, September 2023, pp. 126-142
P- ISSN: 2220-5381
E- ISSN: 2710-1096

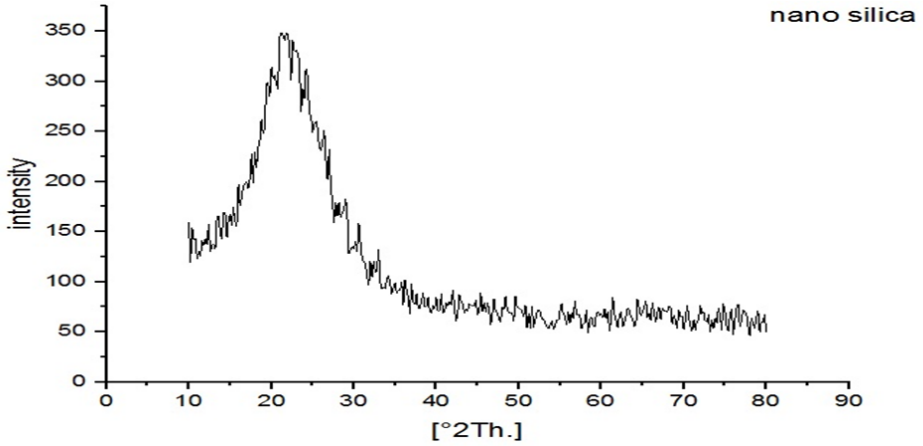

Fig. (3): XRD of nano-silica sampl

3.1.3 AFM

Figure (4) displays a granularity cumulation dispersion chart and an image of particle size distribution in two and three dimensions, revealing aregular particle dimension of 58 nm for the nano-silica produced in this work. Such behavior shows that nano-silica generated using Iraqi sands has a smaller particle size than nano-silica produced from other materials, including those reported by Shnaihej et al. (150 nm).

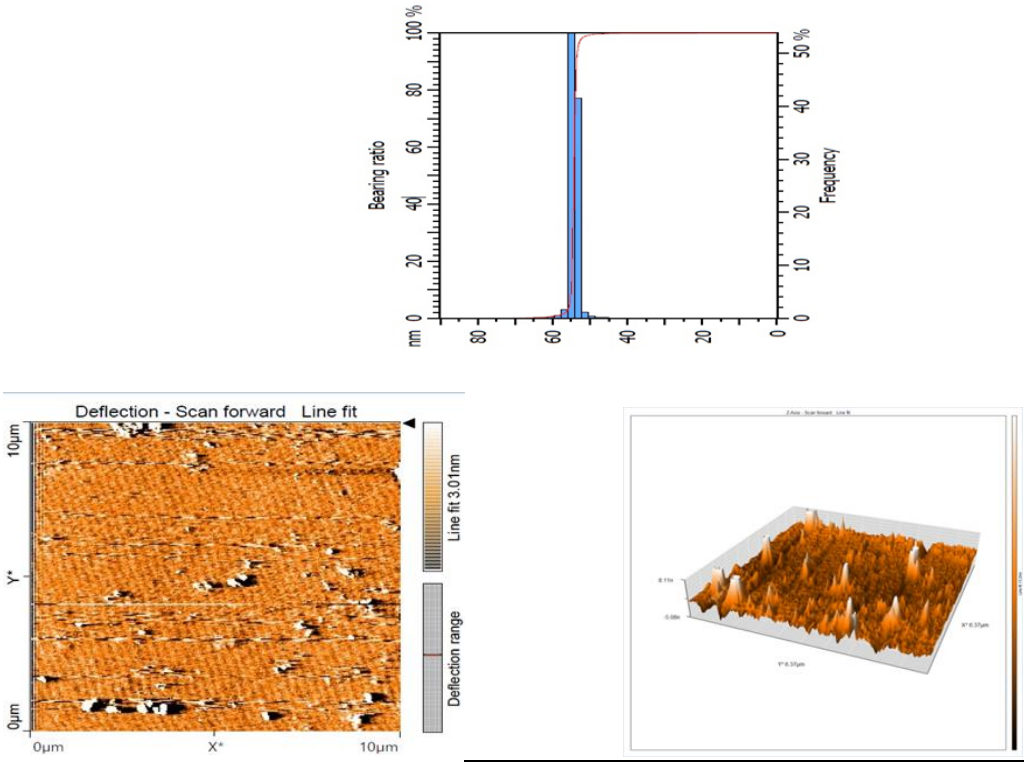

Fig. (4): AFM analysis of nano-silica sample

Open Access
No. 40, September 2023, pp. 126-142
P- ISSN: 2220-5381
E- ISSN: 2710-1096

3.1.4 FT-IR

The FT-IR spectra of the produced nano-silica is depicted in Figure (5). The IR band between 3611 $cm^{-1}$and 3100 cm^{-1} is affected by the stretching vibration of water molecules adsorbed to the silica surface. Similarly, the IR band at 1639 cm^{-1} is caused by the H_2O molecules' bending vibration. The band at 801 $cm^{-1}$is due to the Si-O-Si connection's symmetric stretching vibration. The detected band at 476 cm^{-1} is due to the bond's bending vibration.

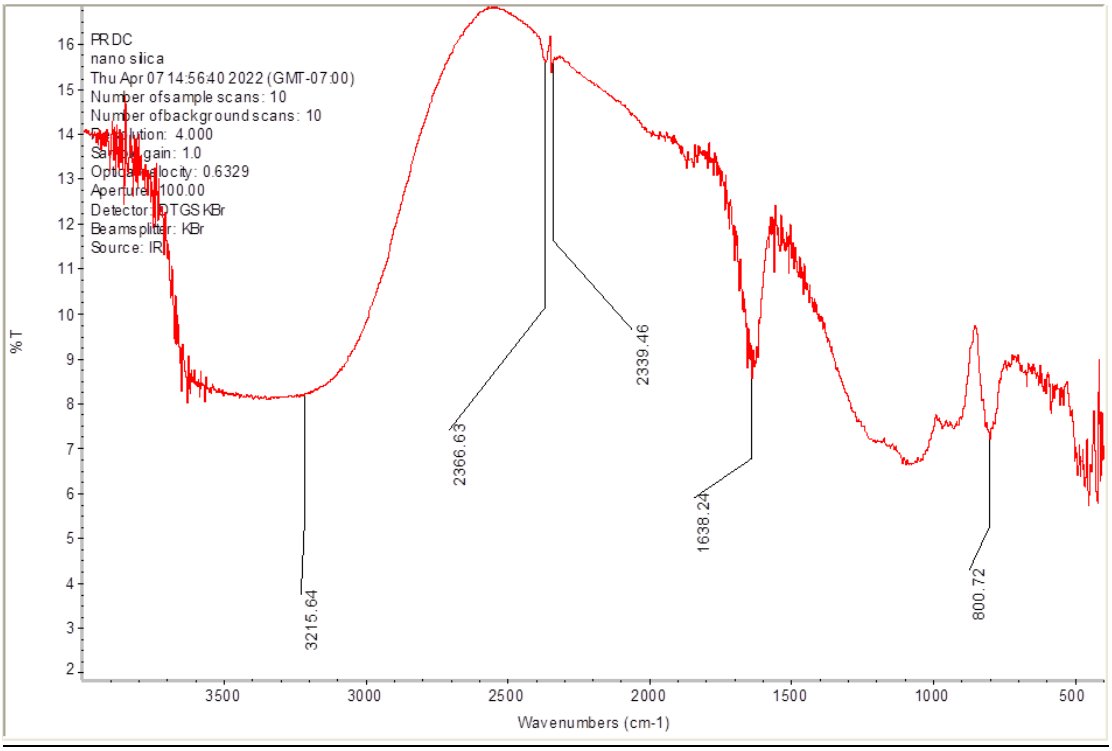

Fig. (5): FTIR spectrum for the prepared nano-silica sample

3.2 Characterization of zeolite Na-MOR

3.2.1 XRD

The X-ray diffractogram pattern of a sample of sodium-based zeolite mordenite (Na-MOR) is displayed in Figure (6). There are zeolite mordenite-specific indexed peaks in 2θ = 12.2, 15.8, 21.4, 23.7, 26.8, 29.6, and 33.9°, showing a high level of crystallization for the band of 2 θ from 0° to 35° for the produced support based on the XRD analysis. Using Scherer's equation, the crystal size L was determined as follows. [16]

$$B(2\theta) = \frac{K\gamma}{L\,cos\theta} \qquad (1)$$

Open Access
No. 40, September 2023, pp. 126-142
P- ISSN: 2220-5381
E- ISSN: 2710-1096

K is the Scherrer's constant, which can range from 0.6 to 2.08 depending on the crystal form; for convenience, we'll assume it to be 1 here; B is the FWHM of the peak at 2θ and ɣ is the center frequency of the spectrum. The X-ray diffractometer uses radiation with a wavelength of (Cu K α, 1.5406). Scherrer's equation applied to X-ray diffraction data yields an average crystal size for Na-MOR of 18.3 nm.

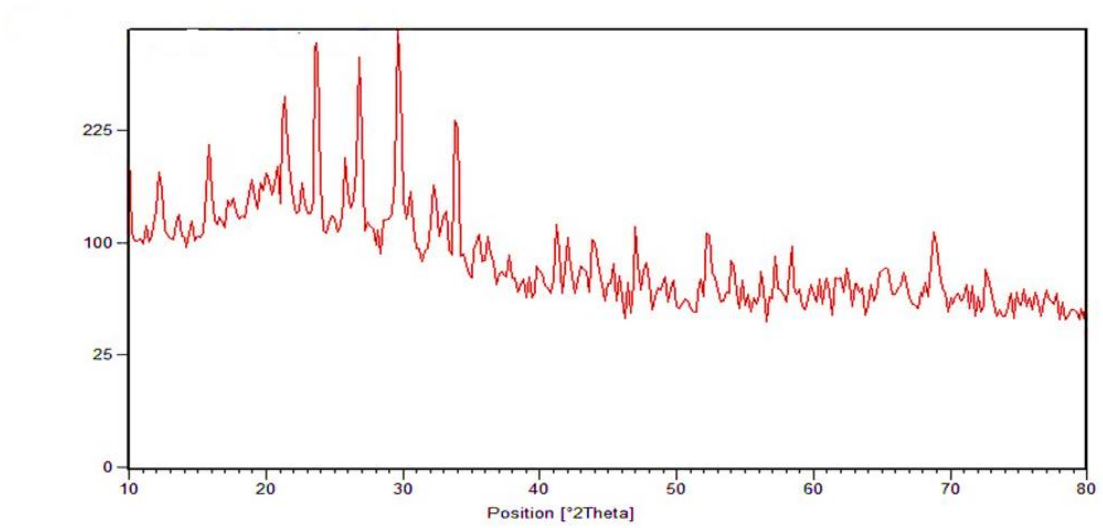

Fig. (6): Na-MOR. zeolite X-ray powder pattern.

3.3 Characterization of H-MOR

3.3.1 XRD

The zeolite's structure was unchanged by the ion exchange and calcination techniques used to generate it in its acidic condition, as show in Figure (7), but the strength of its distinctive peaks increased, indicating an increase in crystallinity HMOR. The intensity of its characteristic reflexes is higher than Na-MOR, which may be explained by the deviation of the Si-O-Al and Al-O bond problems due to structural rearrangement of Si^{+4},Al^{+3}, $H^{+}$to produce the zeolite in the severe stage of structural rearrangement. From XRD data and Scherrer's equation (1), the average crystal size for H–MOR is 31.9 nm.

Open Access
No. 40, September 2023, pp. 126-142
P- ISSN: 2220-5381
E- ISSN: 2710-1096

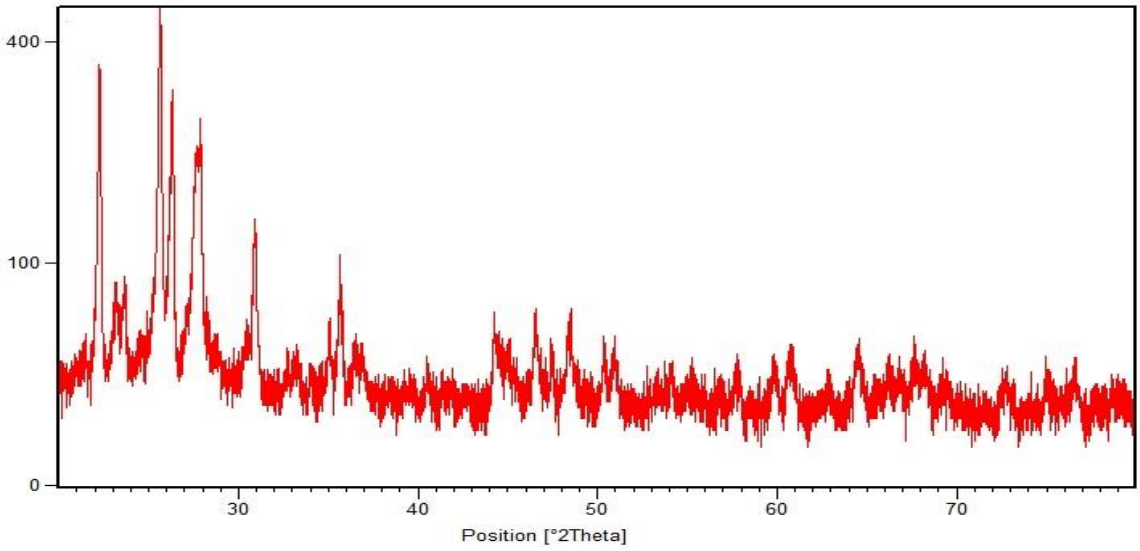

Fig. (7): X-ray of zeolite H-MOR powder

3.3.2 FT-IR

Figure (8) displays the transmittance spectra of H-MOR divided into four key groups: (a) a broad band from 3615 cm^{-1} to 3431 cm^{-1}, which is recognized to the asymmetric stretching of (OH), bonds which represents the presence of moisture; (b) a slight band with intermediate intensity, which is caused by the normal water molecule bending vibration involved with the zeolite framework; and (c) a band at 1225 cm^{-1} which is characteristic The vibration controls the behavior of Si and Al atoms. Finally, (d) an intense peak at about 111cm^{-1} is caused by the interior anti symmetric stretching vibration of the tetrahedral (T-O) bonds. Tetrahedral organization formed the framework of the mordenite**.** [25]. Additionally, the symmetric stretching of (T-O) bonds can be observed as a low-intensity peak at around 624 cm^{-1}. [25]**.**

Open Access
No. 40, September 2023, pp. 126-142
P- ISSN: 2220-5381
E- ISSN: 2710-1096

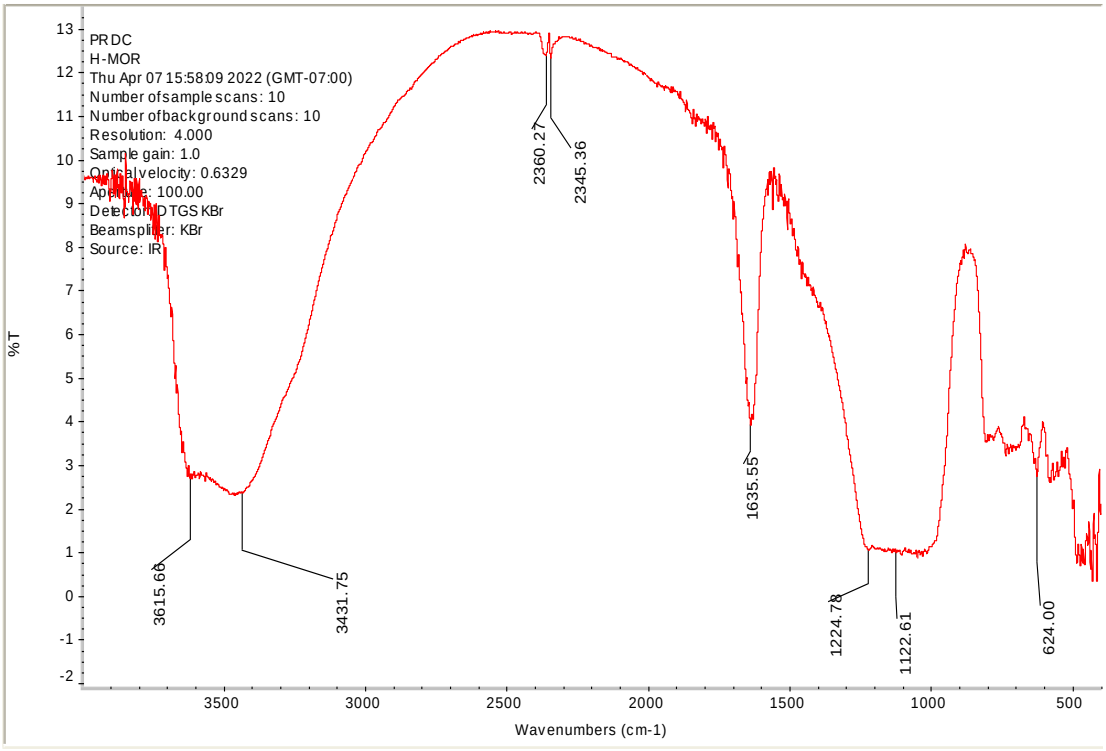

Fig. (8): FTIR spectra of H-MOR, zeolite

3.3.3 BET

The synthesis sample zeolite H-MOR has an overall BET surface area of 205.48m^2/g. Aly et al.(2012) [21] used an inorganic template-free hydrothermal synthesis of a mordenite zeolite with a total specific surface area of 52.14 m^2/g. [21]

3.3.4 FE-SEM

Field Emission Scanning Electron microscopy is used to analyze the surface morphology and structural characteristics of prepared H-MOR zeolite. The FE-SEM pictures in Figure (9), for creating H-MOR, show that this sample contained two phases, a crystalline and an amorphous phase. That plate represents the majority of the crystals. Due to the high quantity of silica, flat and prismatic crystals were seen. Some shapeless silica seemed on the external surface of the crystals. Alternatively, the character of the crystals varied from that of HMOR parent; the supports were lengthier and the character was unequal. The creation of linked and intergrown lath-shaped crystals is visible in the FE-SEM micrograph of the investigated H-MOR. Additionally, the micrograph clearly shows a tiny piece of the crystal band with a peeling habit. Due to their flat plate shape, the particles lead to the formation of mesoporous catalysts.

Open Access
No. 40, September 2023, pp. 126-142
P- ISSN: 2220-5381
E- ISSN: 2710-1096

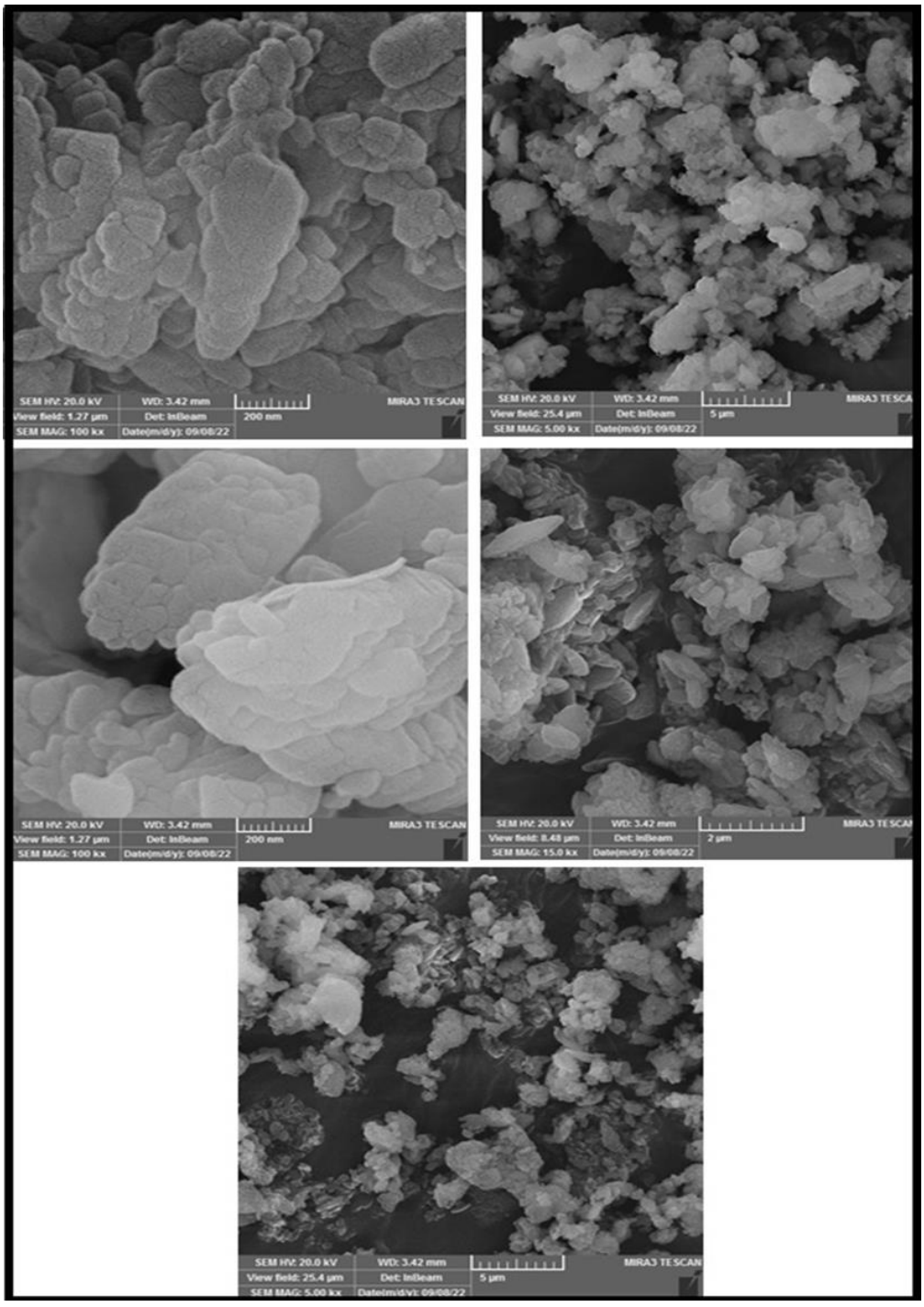

Fig. (9): FE-SEM picture for produced zeolite H-mordenite

3.3.5 XRF analysis for H-MOR and Na-MOR

XRF analyzed Na-MOR zeolite and H-MOR zeolite's elemental makeup was analyzed through XRF. The determined Si/Al ratio is displayed in Table (2). The following is an analysis of the sodium content of the prepared sampler. According to the data in this table, the H-MOR zeolite has no contained sodium at all (0 wt%), indicating that all sodium ions were successfully

Open Access
No. 40, September 2023, pp. 126-142
P- ISSN: 2220-5381
E- ISSN: 2710-1096

exchanged for hydrogen Compared to previous values in the literature [15] [22], the 100% exchange efficiency observed for sodium ions is exceptional. This lead to enhance the acidity of the catalyst to the process that depend on the acidity like isomerization hydrocracking processes.

Table (2) XRF product for composition of prepared mordenite

Zeolite Wt%	Al_2O_3	SO_3	SiO_2	MgO	TiO_2	Na_2O	P_2O_5	Fe_2O_3	Other	Si/Al
Na-MOR	15.9149	0.1965	78.1234	1.8561	0.0303	3.7302	0.0123	0.1084	0.0582	4.9
H-MOR	17.5734	0.2720	79.8914	2.0136	0.0432	ZERO	0.0337	0.1184	0.0543	4.55

4. Conclusion

The mordenite-type zeolites were prepared by using sand from the western part of Iraq (Ar-Rutbah) by SOL-GEL method as a source of silica because of high silica content based on XRF analysis and sodium aluminate as a source of Alumina by the hydrothermal technique at 25 ± 2°C for 7 days, 4N NH_4Cl was used to turn Na-MOR into H-MOR zeolite, exchanging 100% of the Na+ ions.

- The purity of nanosilica produced from Iraqi sand is around 96.7%. Findings indicate that Iraqi sand is a promising raw material for the production of nano silica.
- The composition and the kind of raw material utilized have an important effect on the characteristics of the zeolite materials that are produced
- FE-SEM images of synthesized H-MOR show that plates form the majority of the crystals, which means a high mesopore volume, leading to improved diffusion and convenience for the microspores.
- The 100% exchange efficiency observed for sodium ions is excellent. This lead to enhance the acidity of the catalyst to the process that depend on the acidity like isomerization hydrocracking processes.

It is confirmed that the Iraqi sand has great potential as a different and economical source for the production of nanoslica and zeolite types materials with a good specification.

Open Access
No. 40, September 2023, pp. 126-142
P- ISSN: 2220-5381
E- ISSN: 2710-1096

References

[1] S. Ren, C. Gong, P. Zeng, Q. Guo, and B. Shen, "Synthesis of flammulina-like mordenite using starch as template and high catalytic performance in crack of wax oil," *Fuel*, vol. 166, pp. 347–351, 2016. https://doi.org/10.1016/j.fuel.2015.11.010

[2] L. Tosheva and V. P. Valtchev, "Nanozeolites: synthesis, crystallization mechanism, and applications," *Chem. Mater.*, vol. 17, no. 10, pp. 2494–2513, 2005. https://doi.org/10.1021/cm047908z

[3] M. S. Holm, E. Taarning, K. Egeblad, and C. H. Christensen, "Catalysis with hierarchical zeolites," *Catal. Today*, vol. 168, no. 1, pp. 3–16, 2011. https://doi.org/10.1016/j.cattod.2011.01.007

[4] K. Cao *et al.*, "Organic-free synthesis of MOR nanoassemblies with excellent DME carbonylation performance," *Chinese J. Catal.*, vol. 42, no. 9, pp. 1468–1477, 2021. https://doi.org/10.1016/S1872-2067(20)63777-9

[5] S. Navalon, A. Dhakshinamoorthy, M. Alvaro, M. Antonietti, and H. García, "Active sites on graphene-based materials as metal-free catalysts," *Chem. Soc. Rev.*, vol. 46, no. 15, pp. 4501–4529, 2017. https://doi.org/10.1039/C7CS00156H

[6] M. Tajbakhsh, H. Alinezhad, M. Nasrollahzadeh, and T. A. Kamali, "Preparation, characterization and application of nanosized CuO/HZSM-5 as an efficient and heterogeneous catalyst for the N-formylation of amines at room temperature," *J. Colloid Interface Sci.*, vol. 471, pp. 37–47, 2016. https://doi.org/10.1016/j.jcis.2016.02.062

[7] K. Nakamoto, M. Ohshiro, and T. Kobayashi, "Mordenite zeolite—Polyethersulfone composite fibers developed for decontamination of heavy metal ions," *J. Environ. Chem. Eng.*, vol. 5, no. 1, pp. 513–525, 2017. https://doi.org/10.1016/j.jece.2016.12.031

[8] C. Shao, H.-Y. Kim, J. Gong, B. Ding, D.-R. Lee, and S.-J. Park, "Fiber mats of poly (vinyl alcohol)/silica composite via electrospinning," *Mater. Lett.*, vol. 57, no. 9–10, pp. 1579–1584, 2003. https://doi.org/10.1016/S0167-577X(02)01036-4

[9] M. E. Davis, "Molecular sieves: Principles of synthesis and identification: By R. Szostak.

Open Access
No. 40, September 2023, pp. 126-142
P- ISSN: 2220-5381
E- ISSN: 2710-1096

Van Nostrand-Reinhold, New York, 1988. $69.95." Academic Press, 1989.

[10] R. W. Gosselink, S. L. Sagala, J. D. Meeldijk, P. E. de Jongh, and K. P. de Jong, "Alkaline treatment on commercially available aluminum rich mordenite," *Appl. Catal. A Gen.*, vol. 382, no. 1, pp. 65–72, 2010. https://doi.org/10.1016/j.apcata.2010.04.023

[11] M. Müller, G. Harvey, and R. Prins, "Comparison of the dealumination of zeolites beta, mordenite, ZSM-5 and ferrierite by thermal treatment, leaching with oxalic acid and treatment with SiCl4 by 1H, 29Si and 27Al MAS NMR," *Microporous mesoporous Mater.*, vol. 34, no. 2, pp. 135–147, 2000. https://doi.org/10.1016/S1387-1811(99)00167-5

[12] M. M. Mohamed and T. M. Salama, "Effect of mordenite dealumination on the structure of encapsulated molybdenum catalysts," *J. Colloid Interface Sci.*, vol. 249, no. 1, pp. 104–112, 2002. https://doi.org/10.1006/jcis.2002.8218

[13] M. A. Klunk *et al.*, "Synthesis and characterization of mordenite zeolite from metakaolin and rice husk ash as a source of aluminium and silicon," *Chem. Pap.*, vol. 74, no. 8, pp. 2481–2489, 2020. https://doi.org/10.1007/s11696-020-01095-4.

[14] L. Li *et al.*, "Preparation of Spherical Mordenite Zeolite Assemblies with Excellent Catalytic Performance for Dimethyl Ether Carbonylation," *ACS Appl. Mater. Interfaces*, vol. 10, no. 38, pp. 32239–32246, 2018. https://doi.org/10.1021/acsami.8b11823.

[15] H. M. Hussain and A. A. K. Mohammed, "Preparation and Characterization of mordenite Zeolite from Iraqi Sand," *IOP Conf. Ser. Mater. Sci. Eng.*, vol. 518, no. 6, 2019. https://doi.org/10.1088/1757-899X/518/6/062002.

[16] A. Journal and O. F. Basic, "Synthesis of Mesoporous Mordenite Zeolite by Different Natural Raw Materials," *Aust. J. Basic Appl. Sci.*, vol. 11, no. January, pp. 27–34, 2017.

[17] J. Zhu *et al.*, "Ultrafast, OSDA-free synthesis of mordenite zeolite," *CrystEngComm*, vol. 19, no. 4, pp. 632–640, 2017. https://doi.org/10.1039/C6CE02237E

[18] R. A. Kadhim, A. A. K. Mohammed, and H. M. Hussein, "Synthesis and preparation of Nano-silica particles from Iraqi western region silica sand via SOL-GEL method," *J. Phys. Conf. Ser.*, vol. 1973, no. 1, 2021. https://doi.org/10.1088/1742-6596/1973/1/012071.

Open Access
No. 40, September 2023, pp. 126-142
P- ISSN: 2220-5381
E- ISSN: 2710-1096

[19] H. M. Hussain and A. A.K. Mohammed, "Experimental Study of Iraqi Light Naphtha Isomerization over Ni-Pt/H-Mordenite," *Iraqi J. Chem. Pet. Eng.*, vol. 20, no. 4, pp. 61–66, 2019. https://doi.org/10.31699/ijcpe.2019.4.10.

[20] E. A. Okoronkwo, P. E. Imoisili, S. A. Olubayode, and S. O. O. Olusunle, "Development of Silica Nanoparticle from Corn Cob Ash," *Adv. Nanoparticles*, vol. 05, no. 02, pp. 135–139, 2016. https://doi.org/10.4236/anp.2016.52015.

[21] H. M. Aly, M. E. Moustafa, and E. A. Abdelrahman, "Synthesis of mordenite zeolite in absence of organic template," *Adv. Powder Technol.*, vol. 23, no. 6, pp. 757–760, 2012. https://doi.org/10.1016/j.apt.2011.10.003.

[22] E. T. C. Vogt and B. M. Weckhuysen, "Fluid catalytic cracking: recent developments on the grand old lady of zeolite catalysis," *Chem. Soc. Rev.*, vol. 44, no. 20, pp. 7342–7370, 2015. https://doi.org/10.1039/C5CS00376H